

30 **Abstract**

31 Forest ecosystems are increasingly exposed to the combined pressure of climate change
32 and attacks by pests and pathogens. These stress factors can threaten already vulnerable
33 species triggering dieback and rising defoliation and mortality rates. To characterize
34 abiotic (drought, climate warmings) and biotic (pathogens) risks and their spatiotemporal
35 patterns we quantified the recent loss of vitality for the endangered and relict *Abies*
36 *pinsapo* forests from Andalusia, south-eastern Spain. *Abies pinsapo* is an iconic
37 Mediterranean fir showing a high vulnerability to drought stress and also to several pests
38 (*Cryphalus numidicus*) and root rot fungi (*Armillaria mellea*). We analyzed a monitoring
39 network dataset of radial growth, defoliation and mortality from 2001 to 2017 including
40 1025 trees situated in three major mountain ranges (Sierra de Grazalema, Sierra de las
41 Nieves, and Sierra Bermeja). We fitted several statistical models to determine the main
42 drivers of changes in defoliation, a proxy of tree vigor, and mortality. Defoliation and
43 mortality rates were much higher towards the East of the study area, mirroring the
44 gradient from Atlantic to Mediterranean climatic conditions. In the most affected stands
45 tree defoliation increased in response to a combination of long and severe droughts, with
46 attacks by the beetle *C. numidicus*. Mortality rates increased in response to a higher
47 defoliation rate, a lower relative radial-growth rate, long and severe droughts and a higher
48 incidence of *A. mellea*. Our findings illustrate the value of monitoring networks recording
49 changes in forest health to quantify and forecast future vulnerability of threatened tree
50 species.

51

52 **Keywords:** Forest health, monitoring network, defoliation rate, mortality rate,
53 Mediterranean fir forests.

54 **1. Introduction**

55 Damaging biotic agents and climate change are two of the global-change components
56 tightly interrelated which negatively impact forest health and affect the sustainability of
57 forest resources (Trumbore et al., 2015). For instance, an increasing frequency of extreme
58 climatic events such as droughts has been shown to threaten forest health at a global scale
59 (McDowell et al., 2020). There is also evidence for an increasing impact of forest pests
60 and diseases contributing to changes in forest composition, structure, and ecosystem
61 processes (Ayres and Lombardero, 2000; Cobb and Metz 2017). However, we still do not
62 have full understanding on how forests respond to the interaction between these threats,
63 particularly in small remnants of threatened and vulnerable tree populations. This is due
64 to the complexity of understanding the mechanisms underlying the relationship between
65 forest health and stress factors (Hartmann et al., 2018; Senf et al., 2018; Seidling, 2019).
66 In this context, a loss in forest health and tree vigour may compromise the ability of forest
67 to maintain productivity, long-term sustainability of related ecosystems services, and
68 resilience.

69 Mediterranean fir forests are among the most threatened forest ecosystems in
70 Europe (Linares 2011). For instance, several studies suggest that both abiotic and biotic
71 stress factors significantly reduced radial growth in Mediterranean fir forests, causing
72 extensive defoliation and triggering dieback and mortality events (Sánchez-Salguero et
73 al. 2017; Gazol et al., 2020). This pattern is particularly relevant for those populations
74 located at their southernmost or xeric limit of distribution, where they tend to form
75 fragmented and relict populations. In these stands, additional stress imposed by climate
76 change and droughts may make them more vulnerable to pest and pathogen attacks,
77 ultimately threatening their existence. An emblematic species in this status is the Spanish
78 fir (*Abies pinsapo* Boiss. subsp. *pinsapo*), currently occurring in small mountain areas in

79 Southern Spain (Linares et al. 2010a). Abiotic stress factors such as drought seem to act
80 simultaneously with biotic factors driving *A. pinsapo* forest dynamics (Linares et al.,
81 2010a, 2011). In fact, the co-occurrence of drought and damage related to pests and
82 pathogens such as the root rot fungus *Heterobasidion annosum* (Fr.) Bref. s.l. and the
83 bark beetle *Cryphalus numidicus* (Eichhoff, 1878) have been related to periods of growth
84 decline and high mortality rate of *A. pinsapo* (Navarro-Cerrillo and Calzado, 2004;
85 Linares et al., 2010b). Lately, there is new evidence for the more widespread occurrence
86 and effects of these mortality and defoliation events (Lechuga et al., 2017).

87 Understanding the relevance of the different stress factors driving the
88 phytosanitary status of unique, relict *A. pinsapo* forests is of paramount importance to
89 promote adaptive management strategies towards their conservation. Forest health status
90 is the result of complex mechanisms acting in conjunction. Overall, we expect higher
91 fitness (e.g., increased growth) in those areas where the environmental conditions match
92 the optima for the species (Dobbertin 2005). In contrast, increasing levels of stress proxies
93 such as defoliation and mortality should indicate problems in forest health and
94 productivity (Teshome et al., 2020). Unfortunately, the relationships between these two
95 groups of factors are not always clear, as there might be lagged responses and complex
96 site-dependent effects between abiotic and biotic stress factors.

97 To address these uncertainties, systematic monitoring networks offer a unique
98 source of information providing spatio-temporal information on forest health considering
99 several proxies of tree vigour. Forest health assessment systems and networks are needed
100 to understand current and future changes in biotic and abiotic stress factors and their
101 relationship with tree health (Potter and Conkling, 2017). In Europe, the International
102 Cooperative Programme on Assessment and Monitoring of Air Pollutant Effects on
103 Forests (ICP Forests Network) has been monitoring forest condition using harmonized

104 methods and criteria (Bussotti and Pollastrini, 2017). ICP assessments have allowed
105 compiling detailed cases of forest dieback and growth decline throughout Europe,
106 showing an increased impact of biotic and abiotic stress agents on forest health and
107 ecosystem processes (Ferretti et al, 2014; Seidling, 2019), including drought-prone
108 Mediterranean countries. For instance, in Spain several episodes of defoliation loss and
109 increased mortality have been shown in several conifers (Carnicer et al. 2011; Cruz et al.,
110 2014).

111 Since the late 1990s, large areas of conifer forests in Andalusia (southern Spain)
112 have shown dieback episodes characterized by high levels of defoliation and mortality
113 (Sánchez-Salguero et al. 2012; Cruz et al., 2014). We used Spanish fir forests as study
114 case to understand the critical factors affecting forest health on Mediterranean conifer
115 forests. These forests have been monitored during the period 2001–2017 through an
116 intensive Monitoring Forest Health Network using harmonized ICP methods (Navarro-
117 Cerrillo and Calzado, 2004). This network is a unique setup towards understanding
118 complex mechanisms behind species decline on its whole distribution geographical scale
119 (Axelson et al., 2019). The objective of this research is to describe the current status of
120 health condition of *A. pinsapo* forests and to analyse the temporal trends in defoliation
121 and mortality to identify potential drivers (i.e., climatic, edaphic, dasometric and biotic
122 variables) underlying these processes. Specifically, we aim to: (i) describe the spatial and
123 temporal trends of annual defoliation and mortality rates, (ii) identify the main abiotic
124 and biotic stress factors contributing to mortality and defoliation of *A. pinsapo*, and (iii)
125 understand the relationships between two key forest health indicators (growth and
126 defoliation) driving *A. pinsapo* forest dynamics. We discuss findings in relation to the
127 future stability of *A. pinsapo* forests threatened under global change and suggesting
128 adaptive management and mitigation strategies.

129 **2. Material and Methods**

130 *2.1. Study area*

131 The study area consists of a long, northerly-running ridge located in southwestern Spain
132 (Malaga and Cádiz provinces, Andalusia; 36° 43' N, 4° 58' W) (Fig. 1). The area ranges
133 in elevation from 700 to 1800 m.a.s.l. with *A. pinsapo* occurring mainly in wet or mesic
134 sites. The occurrence of these forests is concentrated in three distinct mountain regions:
135 Sierra de las Nieves (hereafter SN), Sierra Grazalema (hereafter SG) and Sierra Bermeja
136 (hereafter SB) (Fig. 1). These forests are subjected to water deficit in summer from June
137 to September, a typical feature of Mediterranean climate. Average annual precipitation in
138 the area is 1089 mm and mean annual temperature is 11.6 °C. Soils are predominantly
139 calcareous. Most formerly pure *A. pinsapo* forests were converted by long-term human
140 use to mixed forests with evergreen and deciduous oak species (*Quercus ilex* L. subsp.
141 *ballota* (Desf.) Samp. and *Q. faginea* Lam., respectively), and natural and planted
142 Mediterranean pine species (*Pinus halepensis* Mill., *Pinus pinaster* Aiton.).

143

144 *2.2. Forest health diagnosis*

145 In 2001, a Level I forest damage monitoring network (RED PINSAPO) was established
146 according to a systematic sampling design (1×1 km; N=43 plots) (Fig. 1). Plots were of
147 variable radius, and 24 trees were selected according to ICP methodology (6 trees per
148 quadrant, NE, SE, SW and NW) (Eichhorn et al., 2016; Consejería de Medio Ambiente y
149 Ordenación del Territorio, 2018). Plots were dominated by *A. pinsapo* (cover over 50%).
150 Tree diameter at breast height (dbh, measured at 1.3 m) was measured to calculate a
151 relative growth rate from 2001 to 2017 (RGR). Annual monitoring of several variables
152 used to describe tree health was performed on all tagged trees each year in August or
153 September (i.e., crown defoliation and mortality, and biotic and abiotic damages).

154 Defoliation was assessed visually on all the trees present in the plots into one of twenty
155 percentage classes (intervals of 5 units between 0 and 100) in comparison to a local
156 “reference tree” according to Level I ICP Forests standard (Eichhorn et al. 2010) by the
157 same independent team. The use of defoliation as a tree health status condition is a
158 practical convention, even though it cannot be considered a true tree physiological trait
159 (Lorenz and Becher 2013). All dead trees were recorded and substituted by another tree
160 of similar size and sociological status within the plot to estimate plot defoliation with the
161 same number of individuals. For mortality analysis replacement trees were excluded from
162 this study. The number of assessed trees in this period comprised 1025 *A. pinsapo*
163 individuals.

164 The mortality rate was calculated as:

165

$$166 \quad m = \left(1 - \frac{N_{t1}}{N_{t0}}\right)^{\frac{1}{T}} * 100 \quad (1)$$

167 where N_{t1} is the number of trees that survived the census interval (2001-2017), N_{t0} the
168 initial number of trees and T the time span (2001–2017). To provide a better
169 understanding of the spatial drivers of mortality, mortality rates were also calculated for
170 the three distribution areas (SB, SG and SN ranges) (Fig. 1).

171 Biotic and abiotic agents were described using standard symptoms, apparent
172 severity (level of damage and abundance), and the inferred cause (when known) (see ICP
173 Forests 2004). Pest severity was expressed as number of trees damaged in 2017 by several
174 major pathogens or pests including fungi (*Armillaria mellea* (Vahl.: Fr.) Kumm.) and
175 insects (*Cryphalus numidicus* Eich., and *Dioryctria auloi* Barbey). Finally, tree species
176 richness per plot was also obtained (TDv).

177

178

179 *2.4. Environmental variables*

180 The dataset contains several categories of variables: mean climate (e.g., temperature,
181 precipitation), annual climate (temperature, precipitation and drought index), topographic
182 (e.g., slope, aspect), and edaphic conditions (e.g., texture, soil pH) (Table S1,
183 Supplementary Material). All data layers were downloaded from the Andalusian
184 Environmental Information Network – REDIAM
185 (<http://www.juntadeandalucia.es/medioambiente/site/rediam/>). Mean climate (period
186 1971–2000), topographic and edaphic data were extracted from the Forest Biomass
187 project of Andalusia at a 100-m resolution (Table S1, Supplementary Material; see
188 methods at Guzmán-Álvarez et al 2012). Annual climate variables were calculated from
189 monthly precipitation and temperature interpolations of meteorological stations located
190 in Andalusia at 500- and 100-m resolution, respectively. To quantify drought severity, we
191 obtained the Standardised Precipitation-Evapotranspiration Index (SPEI) calculated at
192 18- (SPEI₁₈) and 24-month resolutions (SPEI₂₄) from the SPEI global drought database
193 at a 0.5° resolution (<http://sac.csic.es/spei/index.html>; accessed 12 December 2020).
194 These two periods correspond to mid- and long-term duration droughts. This multi-scalar
195 drought index allows characterizing deviations of normal water-balance conditions by
196 considering changes in precipitation and evapotranspiration rates (Vicente-Serrano et al.
197 2010).

198 Prior to analysis we checked potential collinearity problems among the
199 explanatory variables using the Pearson correlation coefficient (Zuur et al., 2010). We
200 selected variables with a pair-wise correlation lower than 0.6 (Figure S1). From the sets
201 of highly correlated variables, we selected those with the widest use in the literature and
202 clearest biological meaning in relation to the study system (Table S1, Supplementary

203 Material). The final selection included: drought index (24-month long SPEI in summer;
204 SPEI24), average total precipitation (ptt), slope and insolation (ins) of each stand, soil
205 depth (ps) as well as the relative growth rate (RGR) and stand Dbh in 2017 (D2017).
206 Finally, we also considered the pest severity by *Armillaria mellea* (Am), *Cryphalus*
207 *numidicus* (Cn) and *Dioryctria auloi* (Da) and tree diversity of the plot (TDv).

208

209 *2.5. Spatio-temporal patterns of defoliation and mortality rates*

210 Kernel Density Estimation (KDE) was used to assess the spatio-temporal correlation
211 patterns of tree defoliation and mortality rates. This is a non-parametric method which
212 estimates the probability density function of random variables and has been widely used
213 in forest ecology (Wandresen et al., 2019). The distribution patterns of defoliation and
214 mortality rates were explored based on finite data samples (O'Brien et al., 2012), and
215 KDE was calculated for each year of the time series (2001–2017) weighting observations
216 by the number of dead individuals recorded and the defoliation levels. We selected a
217 Gaussian kernel density (KD) function, and the optimal bandwidth was estimated using
218 leave-one-out least-squares cross-validation for bivariate KD bandwidths estimation in
219 the *sparr* R package (Davies et al., 2018).

220

221 *2.6. Relationships between abiotic and biotic stress factors and defoliation*

222 The response function of defoliation with respect to environmental and management
223 variables was studied in each of the monitoring network plots. We applied linear mixed-
224 effects models (Pinheiro and Bates 2000) to study the relationship between stand
225 defoliation and the climatic, topographic and forest related conditions of each stand in the
226 period 2001–2017. Models were created for all sites and for each site, separately
227 (excluding Sierra Bermeja due to the low number of points). We used plot identity as a

228 random factor to account for the longitudinal structure of the data (i.e., defoliation was
229 assessed in the same trees during the study period). Defoliation was log-transformed
230 ($\log(x+1)$) prior to the analyses. As explanatory variables we included all non-collinear
231 variables indicated in previous section. We also considered potential interactions between
232 the drought index and other variables (see full model variables in table S3). To determine
233 the impact in the results of outliers and extreme values, we evaluated the fit of the model
234 graphically by examining the residuals and the fitted values (Zuur et al. 2010).

235 The resulting models that were generated with the different combinations of the
236 explanatory variables were ranked according to the second order Akaike Information
237 Criterion (AICc). The Δ AICc of each model was calculated as the difference between the
238 AICc of each model and the minimum AICc found for the set of models. The Δ AICc can
239 be used to select those models that best explain the response variable because those Δ AIC
240 values lower than 2 indicate the suitability of the selected model while values above 7
241 indicate a poor fit as compared to the best model (Burnham and Anderson 2002). The
242 relative importance of the explanatory variables included in the selected models was
243 calculated based on the Akaike weights of each model. For each variable, the importance
244 is calculated as the sum of model weights over all models including each variable. The
245 larger the importance of the models in which the variable is present the more relative
246 importance the variable has.

247 Model comparison and averaging were used to select the best model and to assess
248 the relative importance of each variable (Burnham and Anderson 2002). After selecting
249 those models having a Δ AICc lower than 10 (i.e., the best models), the coefficients for
250 each one of the explanatory covariates included in the model were estimated by means of
251 model averaging. To elucidate potential influences of outliers and extreme values, we

252 evaluated the fit of the model by graphical examination of the residuals and the fitted
253 values (Zuur et al. 2010).

254 Statistical analyses were carried out in the R environment v 3.6.3 (R Core Team,
255 2020). The “lme” function of the *nlme* package was used to fit the linear mixed-effects
256 models (Pinheiro et al., 2014). The *MuMIn* package was used to perform the multi-model
257 selection (Barton 2012). The *visreg* package was used to visualize results of the linear
258 mixed-effect models (Breheny and Burchett 2017).

259

260 *2.7. Models of mortality rates*

261 We studied the variability of mortality rates across regions and environmental factors
262 with a combination of different analyses. First, we calculated the mortality time series for
263 each individual tree. It comprised the number of years from the year of plot establishment
264 (2001) to the date of tree death (up to 2017). Second, we used the Kaplan-Meier
265 estimation method to create tree survival curves and to determine the unadjusted
266 probabilities of survival (with associated 95% confidence intervals) for the studied period
267 (2001–2017). Chi-squared test was performed to determine if significant differences were
268 present among the survival probability of each mountain region, and pairwise multiple
269 comparison adjustment with the Bonferroni’s correction was used to test differences
270 between groups (Logan et al., 2005). Third, we explored the relation between mortality
271 (i.e. time to death) and the three sets of non-collinear variables (i.e. tree level
272 characteristics, health status and site conditions) using Cox proportional hazard models
273 (Cox 1972). As trees were nested in plots, we controlled by plot id using two separate
274 methods, clustering and random effect (O’Quigley and Stare 2002). As results were
275 similar, we present for simplicity the clustering method. We implemented separate
276 models for each group of variables and all combined. For each model we performed an

277 automatic selection of variables based on AIC following a similar procedure that
278 Esquivel-Muelbert et al. (2020). Finally, we carried out and compared separate cox
279 proportional hazard models for the two mountain regions with mortality (SG and SN).
280 These analyses were performed using the following R packages: *stats*, *survival*,
281 *survminer*, *ggplot2*, *ggfortify*, and *ranger* (Kassambara and Kosinski, 2018; Therneau and
282 Grambsch, 2000).

283

284 **3. Results**

285 *3.1. Spatial and temporal trends in defoliation and mortality rates*

286 Defoliation and mortality rates varied significantly across the distribution of *A. pinsapo*
287 (Figs. 2 to 4, Supplementary Table S2). At the distribution area, defoliation (mean±SD)
288 slightly increased from 2001 ($D_{2001}=16.67\pm 1.66\%$) to 2017 ($D_{2017}=19.94\pm 1.09\%$),
289 decreasing in SB ($D_{2017}=13.12\pm 2.24\%$), and increasing in SG ($D_{2017}=18.64\pm 3.88\%$), and
290 SN ($D_{2017}=20.98\pm 0.98\%$). Defoliation of *A. pinsapo* showed a clear spatial pattern,
291 increasing from western sites (SB) to the northeast (SN) (Fig. 4).

292 Mortality was also higher in SN ($1.03\pm 0.30\%$ year⁻¹) than in SG ($0.74\pm 0.28\%$
293 year⁻¹), with high differences until the year 2012, but without significant differences at
294 the end of the period ($P=0.272$) (Fig. 3). In SG we noticed a significant change in the
295 mortality trend after this year, meanwhile the mortality trend was stable over the whole
296 period in SN. There was not mortality in SB during the time span of this study. Similarly,
297 the KDE approach highlighted some areas in SN with high mortality rates, with lower
298 incidence in SG and no mortality in SB (Fig. 4).

299

300

301 3.2. Models of tree defoliation

302 Defoliation did not differ significantly ($P < 0.01$) between sites (Table S2 Supplementary
303 Material). *A. pinsapo* defoliation was not directly associated with any of the tree, health
304 or site factors considered (Table 1). We only found a significant interaction between the
305 presence of *C. numidicus* and long-term droughts (SPEI₂₄) (Table 1), indicating that
306 higher defoliation levels appeared at the combination of higher pest and drought levels
307 (Fig. 5).

308

309 3.3. Models of mortality rate

310 Tree mortality rates significantly differed among zones according to the Kaplan-Meier
311 analysis (Fig. 3; $\chi^2 = 11$, $P < 0.01$). *A. pinsapo* mortality risk across the species distribution
312 area depended on the characteristics of tree-level attributes, health status and site
313 conditions (Table 2). Mortality models including all traits performed better than models
314 with either group of risk factors alone (Table 2). Models with only health plot status traits
315 predict mortality better than models containing only tree-level attributes (Table 2).

316 Relative growth rates, defoliation changes and damage by *A. mellea* were the best
317 predictors of tree mortality (Table 3). Specifically, we found higher mortality risk for
318 slow growing trees, with defoliation above 50%, high occurrence of *A. mellea* and after
319 drought events (Fig. 6). Patterns were similar across sites, although the relevance of
320 variables varied (Fig. 6, Table S7). In SN fast growing trees with higher defoliation were
321 at higher risk, whilst in SG pests, mid-term droughts (SPEI₁₈) and tree diversity impacted
322 mortality (Table S7). Pest and pathogen incidence interacted significantly with tree and
323 site factors (Table 3). Specifically, *A. mellea* and *C. numidicus* produced higher mortality
324 risk at higher insolation levels.

325

326 **4. Discussion**

327 We provide here the first comprehensive, spatio-temporal assessment of *A. pinsapo*
328 mortality and defoliation based on a systematic health monitoring network. Previous
329 studies of health status in these forests have been highly localized or restricted to a small
330 number of plots (Linares et al., 2009, 2010a; Lechuga et al. 2017). We show that a
331 combination of stress factors is likely to be the most common cause of defoliation and
332 mortality across the species distribution area in southern Spain. This is in line with
333 previous studies showing how elevated tree mortality rates are one of the main symptoms
334 of climate change impact on drought-prone *A. pinsapo* forests (Linares et al., 2009, 2011,
335 Navarro-Cerrillo et al., 2020a).

336

337 *4.1. Spatial and temporal trends of defoliation and mortality rates*

338 Species-oriented forest health networks can describe the spatial and temporal patterns of
339 tree defoliation and mortality over large areas (Carnicer et al., 2011) but also the
340 characteristic health patterns of forest ecosystems of regional concern (Duque Lazo et al.,
341 2017; Sánchez-Cuesta et al., 2021). This information is of paramount importance for
342 vulnerable populations situated at the geographic or climatic edges of their distribution
343 or in xeric areas which are under high risk of being impacted by severe and long droughts.
344 Specifically for *A. pinsapo*, we observed a consistent pattern in defoliation and mortality
345 rates, which were higher in the North Eastern part of the study area (i.e. Sierra de las
346 Nieves) and related to drought and key pest damages. In the other locations (Sierra
347 Bermeja and Sierra de Grazalema) defoliation and mortality rates were lower, and health
348 drivers could not be identified. These contrasting findings across regions coincide with
349 the dissimilar bioclimate types developed for *A. pinsapo* (Fernández Cancio et al. 2007).

350 Sierra de Grazalema and Bermeja locations show a clear Atlantic influence in comparison
351 with the Mediterranean character of the highly affected Sierra de las Nieves. The higher
352 mortality and defoliation rates spreading to the east during the study period, partially
353 agree with previous studies based on species distribution models (Fernández-Cancio et
354 al., 2007; López-Tirado and Hidalgo, 2014; Navarro-Cerrillo et al., 2021), which reported
355 a rapid reduction of the optimal areas for *A. pinsapo* in Sierra de las Nieves, probably
356 connected with a decrease of Mediterranean convective conditions.

357

358 4.2. Drivers of defoliation rates

359 The annual defoliation rate of *A. pinsapo* showed moderate average values (17.6%),
360 similar or slightly lower to those obtained for other European tree species (Klap et al.,
361 2000; Cruz et al., 2014; Michel et al. 2014). The increasing defoliation trend showed here
362 has been also identified in the European ICP Network for the most abundant tree species
363 (Fischer et al., 2010). Particularly, defoliation of *A. pinsapo* was enhanced by an
364 interaction of long droughts and damage related to attacks by the bark beetle *C.*
365 *numidicus*. These results are consistent with spatial distribution models which identified
366 drought-related climatic variables and microclimatic drivers (e.g., aspect) among the most
367 relevant factors to explain current *A. pinsapo* distribution (Navarro-Cerrillo et al., 2021).

368

369 4.3. Drivers of mortality rates

370 Tree mortality is one of the most relevant variables assessed by European forest condition
371 networks (Lorenz and Becher 2013; Neumann et al., 2017). Our empirical results from
372 the *A. pinsapo* monitoring network show high values of accumulated tree mortality
373 (11.53%), and mortality rates (0.90% year⁻¹), significantly higher than that obtained from
374 other forest health networks (0.010-0.015% year⁻¹, Van Mantgem and Stephenson, 2007)

375 and other Mediterranean species (e.g., *Q. ilex*, 0.153%) in southern Spain (Sánchez-
376 Cuesta et al., 2021). High *A. pinsapo* mortality rates have been related to biotic (Navarro-
377 Cerrillo et al. 2003; Sánchez et al., 2007) and abiotic stress factors (Linares et al., 2010
378 a) such as pests, pathogens and drought. In our study, mortality was higher for slow
379 growing trees, with defoliation above 50%, high occurrence of *A. mellea* and after major
380 drought events. Tree diversity was not a significant factor, but recent studies have
381 highlighted the relationship between drought impacts in forests and functional diversity
382 modulating, among others ecosystem functions, their vulnerability to climate-related
383 stresses (see Grossiord, 2020). It should be better investigated if more diverse
384 neighbourhoods increase functional diversity and buffer or provide resilience to *A.*
385 *pinsapo* as it has been indicated for *A. alba* during drought (Gazol and Camarero 2016).

386 Mortality risk increased with the occurrence of pathogenic fungi such as *A. mellea*
387 and the insect *C. numidicus*. Both biotic agents are extremely relevant in the dynamic of
388 *A. pinsapo* forests, particularly under stressing abiotic conditions (Arista et al. 1997).
389 Specifically, we found higher mortality rates when these biotic agents occurred in sites
390 of high insolation. We hypothesized that in these highly exposed areas (e.g. southern
391 slope and higher altitudes) *A. pinsapo* is more vulnerable to the attack of pests, eventually
392 producing mortality events. Other possible causes of the increase in mortality not studied
393 here is the incidence of other pathogenic fungi such as *Heterobasidium annosum* (De Vita
394 et al., 2010); or complex interactions (senescence with age, lack of suitable management,
395 etc., Lechuga et al., 2017). Despite multiple causality of mortality, our results highlight
396 some of the most relevant drivers of mortality on *A. pinsapo* forests, which can provide a
397 better understanding of Spanish fir mortality.

398

399 Forest and natural resource managers must develop new adaptive strategies to
400 respond to climatic changes (Nocentini et al., 2017). Those strategies should be supported
401 by relevant information on observed and projected climate impacts. Regional and local
402 forest health monitoring networks supply on-the-ground forest data for operational-scale
403 adaptation measures to adapt forest ecosystems to climate change (Gustafson et al., 2020).
404 Our results showed some key element for an adaptive silviculture for climate change on
405 *A. pinsapo* forests: control of high-risk pests or maps of mortality pattern to orient the
406 establishment of operational-scale adaptation plots to test specific ecosystem adaptation
407 treatments to climate change through a gradient of adaptive approaches. Those actions
408 contribute to integrate new conceptual tools and processes into silvicultural decisions and
409 management in a context of climate change.

410 **5. Conclusions**

411 Regional and local forest-health monitoring networks are useful tools to provide robust
412 data field changes in vigour and health of vulnerable tree species as we illustrated with
413 the iconic Mediterranean fir *A. pinsapo*. The data recorded in the Spanish fir monitoring
414 network allowed recording changes in forest health condition and assessing cause-effect
415 relationships between tree status (defoliation and mortality), abiotic (drought,
416 topography) and biotic (pests, pathogens) stress factors. Our results show that areas in the
417 north-east part on the *A. pinsapo* distribution (Sierra de las Nieves) have shown increasing
418 defoliation and mortality rates, which were overall related to drought severity, radial-
419 growth loss and damage caused by pests and pathogens (*Armillaria mellea* and *Cryphalus*
420 *numidicus*). Those processes seem to be related to two major stress factors: first, the
421 increase of the aridity gradient from west to east areas influenced by different atmospheric
422 patterns from the Atlantic Ocean and the Mediterranean Sea, respectively; and second,
423 the spread and increase of severity of forest pest and diseases during the last decades

424 (Navarro-Cerrillo et al., 2020b). Drought is supposed to be a predisposing factor which
425 forces the sensitivity to other biotic and abiotic stress factors (Manion and Lachance,
426 1992). Those biotic stressors such as fungi of *Armillaria* species or beetles have been
427 featured as major damage agents in other conifer forests (Müller et al., 2018). Finally,
428 there are very few studies considering the impact of atmospheric pollutants over time, but
429 some reports conclude that it could be also important to explain *A. pinsapo* defoliation
430 (Blanes et al., 2013). Therefore, a continuous increase in *A. pinsapo* dieback incidence
431 can be expected in the coming years in the most defoliated areas (Sierras de las Nieves)
432 as has been illustrated under different growing conditions (Linares et al., 2009, 2011;
433 Navarro-Cerrillo et al., 2020b). Future monitoring efforts must consider ecosystem
434 function and stressor–indicator relationships within the framework of an appropriate
435 statistical design.

436

437 **Acknowledgments**

438 The authors thank the Ministerio de Ciencia, Innovación y Universidades (Spain), for
439 providing the necessary financial support for this study through the ESPECTRAMED
440 (CGL2017-86161-R), ISO-PINE (UCO-1265298) and SilvAdapt RED2018 102719 T
441 projects. PGM was supported by a “Juan de la Cierva-Incorporación” contract (MINECO,
442 IJCI-2017-31733) and FJR-G was supported by a post-doctoral fellowship of the Junta
443 de Andalucía (Spain) and the European Social Fund 2014-2020 Program (DOC_0055).
444 We would like to thank to José López Quintanilla, Angel Carrasco Gotarredona, José
445 Manuel Ruiz Navarro and Sixto Rodriguez as well as all SEDA Network team (Consejería
446 de Agricultura, Pesca y Desarrollo Sostenible, Andalusia Govt.) for their assistance in
447 field work and other contributions to this study. We also acknowledge the institutional
448 support of Campus de Excelencia CeIA3.

449 **6. References**

- 450 Arista, M., Herrera, F.J. & Talavera, S. (1997) *Biología del Pinsapo*. Junta de Andalucía,
451 Consejería del Medio Ambiente, Seville, Spain.
- 452 Axelson, J., Battles, J., Bulaon, B., Cluck, D., Cousins, S., Cox, L., Hood, S., 2019. The
453 California tree mortality data collection network—Enhanced communication and
454 collaboration among scientists and stakeholders. *Calif. Agric.* 73(2), 55-62.
- 455 Ayres, M.P., Lombardero, M.J., 2000. Assessing the consequences of global change for
456 forest disturbance from herbivores and pathogens. *Sci Total Environ.* 262(3), 263-86.
- 457 Barton, K., 2012 MuMIn: multi-model inference. R package version 1.0.0. Available at:
458 <http://CRAN.R-project.org/package=MuMIn>.
- 459 Blanes, M.C., Viñepla, B., Salido, M.T., Carreira, J.A., 2013. Coupled soil-availability
460 and tree-limitation nutritional shifts induced by N deposition: insights from N to P
461 relationships in *Abies pinsapo* forests. *Plant Soil* 366(1-2), 67-81.
- 462 Breheny, P., Burchett, W., 2017. Visualization of regression models using visreg. *R J.* 9,
463 56–71.
- 464 Burnham, K.P., Anderson, D.R., 2002. *Model Selection and Multimodel Inference: a*
465 *Practical Information-Theoretic Approach*, 2nd edn. Springer-Verlag, New York.
- 466 Bussotti, F., Pollastrini, M., 2017. Observing climate change impacts on European
467 forests: what works and what does not in ongoing long-term monitoring networks.
468 *Front. Plant Sci.* 8, 629.
- 469 Carnicer, J., Coll, M., Ninyerola, M., Pons, X., Sánchez, G., Peñuelas, J., 2011.
470 Widespread crown condition decline, food web disruption, and amplified tree
471 mortality with increased climate change-type drought. *P.N.A.S.* 108(4), 1474-1478.
- 472 Cobb, R.C., Metz, M.R., 2017. Tree diseases as a cause and consequence of interacting
473 forest disturbances. *Forests* 8(5), 147.

474 Consejería de Medio Ambiente y Ordenación del Territorio, 2018. Manual para el
475 establecimiento y la evaluación de las parcelas de la Red Andaluza de Seguimiento de
476 Daños sobre Ecosistemas Forestales: Red SEDA y Red de PINSAPO. Junta de
477 Andalucía, Sevilla, Spain.

478 Cox, D. R. (1972). Regression models and life-tables. *J R Stat Soc Series B Stat*
479 *Methodol.* 34(2), 187-202.

480 Cruz, A., Gil, P. M., Fernández-Cancio, Á., Minaya, M., Navarro-Cerrillo, R.M.,
481 Sánchez-Salguero, R., Grau, J.M., 2014. Defoliation triggered by climate induced
482 effects in Spanish ICP Forests monitoring plots. *Forest Ecol. Manag.* 331, 245-255.

483 Davies, T.M., Marshall, J.C., Hazelton, M.L., 2018. Tutorial on kernel estimation of
484 continuous spatial and spatiotemporal relative risk. *Stats. Med.*, 37(7), 1191-1221.

485 De Vita, P., Serrano, M.S., Luchi, N., Capretti, P., Trapero, A., Sánchez, M.E., 2010.
486 Susceptibility of *Abies pinsapo* and its tree cohort species to *Heterobasidion*
487 *abietinum*. *For. Pathol.* 40(2), 129-132.

488 Dobbertin, M., 2005. Tree growth as indicator of tree vitality and of tree reaction to
489 environmental stress: a review. *Eur. J. Forest Res.* 124, 319-333.

490 Duque-Lazo, J., Navarro-Cerrillo, R.M., 2017. What to save, the host or the pest? The
491 spatial distribution of xylophage insects within the Mediterranean oak woodlands of
492 Southwestern Spain. *Forest Ecol. Manag.* 392, 90–104.

493 Eichhorn, J., Roskams, P., Ferretti, M., Mues, V., Szepesi, A., 2016. Visual assessment
494 of crown condition and damaging agents. Manual Part IV, in: Manual on methods and
495 criteria for harmonized sampling, assessment, monitoring and analysis of the effects
496 of air pollution on forests. UNECE ICP Forests Programme Co-ordinating Centre,
497 Eberswalde, Germany, p. 49.

498 Esquivel-Muelbert, A., Phillips, O.L., Brienen, R.J., Fauset, S., Sullivan, M.J., Baker,
499 T.R., Chao, K.J., Feldpausch, T.R., Gloor, E., Higuchi, N., Houwing-Duistermaat, J.,
500 Lloyd, J., Liu, H., Malhi, Y., Marimon, B., Marimon Junior, B.H., Monteagudo-
501 Mendoza, A., Poorter, L., Silveira, M., Galbraith, D., 2020. Tree mode of death and
502 mortality risk factors across Amazon forests. *Nat. Commun.* 11(1), 5515.

503 Fernández-Cancio, A., NavarroCerrillo, R.M., Fernández, R.F., Hernández, P.G.,
504 Meneéndez, E.M., Martínez, C.C., 2007. Climate classification of *Abies pinsapo*
505 Boiss. forests in Southern Spain. *Forest Syst.* 16(3), 222-229.

506 Ferretti, M., Nicolas, M., Bacaro, G., Brunialti, G., Calderisi, M., Croisé, L., Frati, L.,
507 Lanier, M., Maccherini, S., Santi, E., Ulrich, E., 2014. Plot-scale modelling to detect
508 size, extent, and correlates of changes in tree defoliation in French high forests. *Forest*
509 *Ecol. Manag.* 311, 56-69.

510 Fischer, R., Lorenz, M., Granke, O., Mues, V., Iost, S., Van Dobben, H., De Vries, W.,
511 2010. Forest condition in Europe. Institute for World Forestry, Hamburg, Germany.

512 Gazol, A., Camarero, J.J., 2016. Functional diversity enhances silver fir growth resilience
513 to an extreme drought. *J. Ecol.* 104, 1063-1075.

514 Gazol, A., Sangüesa-Barreda, G., Camarero, J.J., 2020. Forecasting forest vulnerability
515 to drought in Pyrenean Silver fir forests showing dieback. *Front. For. Glob. Change* 3,
516 36.

517 Gustafson, E. J., Kern, C. C., Miranda, B. R., Sturtevant, B. R., Bronson, D. R., Kabrick,
518 J. M. (2020). Climate adaptive silviculture strategies: How do they impact growth,
519 yield, diversity and value in forested landscapes?. *Forest Ecol. Manag.* 470, 118208.

520 Grossiord, C., 2020. Having the right neighbors: how tree species diversity modulates
521 drought impacts on forests. *New Phytol.* 228(1), 42-49.

522 Guzman-Álvarez, J.R., Troncoso, J.V., Rengel, A., Sillero, M.L., Álvarez, J.A., Guerrero
523 Álvarez, J.J., Sánchez, R., 2012. Biomasa Forestal en Andalucía. Consejería de Medio
524 Ambiente, Junta de Andalucía.

525 Hartmann, H., Schuldt, B., Sanders, T.G., Macinnis- Ng, C., Boehmer, H.J., Allen, C.D.,
526 Ruehr, N.K., 2018. Monitoring global tree mortality patterns and trends. Report from
527 the VW symposium ‘Crossing scales and disciplines to identify global trends of tree
528 mortality as indicators of forest health’. *New Phytol.* 217(3), 984-987.

529 ICP Forests, 2004. International Co-operative Programme on Assessment and Monitoring
530 of Air Pollution Effects on Forests operating under the UNECE Convention on Long-
531 range Transboundary Air Pollution. <http://icp-forests.net/>

532 Kassambara, A., Kosinski, M., 2018. *Survminer: drawing survival curves using*
533 *“ggplot2.”* Available online: [https://cran.r-](https://cran.r-project.org/web/packages/survminer/survminer.pdf)
534 [project.org/web/packages/survminer/survminer.pdf](https://cran.r-project.org/web/packages/survminer/survminer.pdf) (accessed on 10 February 2021)

535 Klap, J.M., Voshaar, J.H., De Vries, W., Erisman, J.W., 2000. Effects of environmental
536 stress on forest crown condition in Europe. Part IV: statistical analysis of relationships.
537 *Water Air Soil Pollut.* 119(1), 387-420.

538 Lechuga, V., Carraro, V., Viñepla, B., Carreira, J.A., Linares, J.C., 2017. Managing
539 drought-sensitive forests under global change. Low competition enhances long-term
540 growth and water uptake in *Abies pinsapo*. *Forest Ecol. Manag.*, 406, 72-82.

541 Linares JC (2011) Biogeography and evolution of *Abies* (Pinaceae) in the Mediterranean
542 Basin. The roles of long-term climatic changes and glacial refugia. *J. Biogeogr.*, 38,
543 619–630

544 Linares J.C., Camarero, J.J., Carreira, J.A. 2009. Interacting effects of climate and forest-
545 cover changes on mortality and growth of the southernmost European fir forests.
546 *Global Ecol. Biogeogr.* 18: 485-497.

547 Linares, J.C., Camarero, J.J., Carreira, J.A., 2010a. Competition modulates the adaptation
548 capacity of forests to climatic stress: insights from recent growth decline and death in
549 relict stands of the Mediterranean fir *Abies pinsapo*. *J. Ecol.*, 98(3), 592-603.

550 Linares, J.C., Camarero, J.J., Bowker, M.A., Ochoa, V., Carreira, J.A., 2010b. Stand-
551 structural effects on *Heterobasidion abietinum*-related mortality following drought
552 events in *Abies pinsapo*. *Oecologia* 164 (4), 1107-1119.

553 Linares, J.C., Delgado-Huertas, A., Carreira, J.A., 2011. Climatic trends and different
554 drought adaptive capacity and vulnerability in a mixed *Abies pinsapo*–*Pinus*
555 *halepensis* forest. *Clim. Chang.*, 105(1-2), 67-90.

556 Logan, B.R., Wang, H., Zhang, M.J., 2005. Pairwise multiple comparison adjustment in
557 survival analysis. *Statist. Med.* 24, 2509–2523.

558 López-Tirado, J., Hidalgo, P.J., 2014. A high resolution predictive model for relict trees
559 in the Mediterranean-mountain forests (*Pinus sylvestris* L., *P. nigra* Arnold and *Abies*
560 *pinsapo* Boiss.) from the south of Spain: A reliable management tool for reforestation.
561 *Forest Ecol. Manag.* 330, 105-114.

562 Lorenz, M., Becher, G., 2013: Forest Condition in Europe, 2013. Technical Report of ICP
563 Forests. Work Report of the Thünen Institute for World Forestry 2013/1. ICP Forests,
564 Hamburg.

565 Manion, P.D., Lachance, D., 1992. Forest Decline Concepts. APS Press.

566 McDowell, N.G., Allen, C.D., Anderson-Teixeira, K., Aukema, B.H., Bond-Lamberty,
567 B., Chini, L., Hurtt, G.C., 2020. Pervasive shifts in forest dynamics in a changing
568 world. *Science* 368, 6494.

569 Michel, A., Seidling, W., Lorenz, M., Becher, G., 2014. Forest Condition in Europe: 2013
570 Technical Report of ICP Forests; Report under the UNECE Convention on Long-

571 Range Transboundary Air Pollution (CLRTAP). Eberswalde; Hamburg: Johann
572 Heinrich von Thünen-Institut, 134 p, Thünen Working Paper 19.

573 Müller, M. M., Henttonen, H. M., Penttilä, R., Kulju, M., Helo, T., Kaitera, J., 2018.
574 Distribution of *Heterobasidion* butt rot in northern Finland. Forest Ecol. Manag. 425,
575 85-91.

576 Navarro Cerrillo, R.M., Calzado Martínez, C., 2004. Establecimiento de una red de
577 equilibrios biológicos en ecosistemas con presencia de pinsapo (*Abies pinsapo* Boiss.)
578 en Andalucía. Pirineos 158-159, 107-125.

579 Navarro-Cerrillo, R.M., Calzado, C, Quintanilla, J.L., Trapero Casas, A., 2003. Censo de
580 focos de *Heterobasidion annosum* (Fr.) Bref. en ecosistemas de pinsapo. Bol. San.
581 Veg. Plagas 29(4), 581-592.

582 Navarro-Cerrillo, R.M., Camarero, J.J., Manzanedo, R.D., Sánchez-Cuesta, R., Lopez
583 Quintanilla, J., Sanchez Salguero, R., 2014. Regeneration of *Abies pinsapo* within
584 gaps created by *Heterobasidion annosum*-induced tree mortality in southern Spain.
585 Iforest 7(4), 209.

586 Navarro-Cerrillo, R.M., Gazol, A., Rodríguez-Vallejo, C., Manzanedo, R.D., Palacios-
587 Rodríguez, G., Camarero, J.J., 2020 a. Linkages between Climate, Radial Growth and
588 Defoliation in *Abies pinsapo* Forests from Southern Spain. Forests, 11(9), 1002.

589 Navarro Cerrillo, R.M., Duque-Lazo, J., Rios-Gil, N., Guerrero-Alvarez, J.J., Lopez-
590 Quintanilla, J., Palacios-Rodriguez, G., 2021. Can habitat prediction models contribute
591 to the restoration and conservation of the threatened tree *Abies pinsapo* Boiss. in
592 Southern Spain?. New Forests, 52(1).

593 Navarro-Cerrillo, R.M., Manzanedo, R.D., Rodriguez-Vallejo, C., Gazol, A., Palacios-
594 Rodríguez, G., Camarero, J.J., 2020c. Competition modulates the response of growth

595 to climate in pure and mixed *Abies pinsapo* subsp. *maroccana* forests in northern
596 Morocco. *Forest Ecol. Manag.* 459, 117847.

597 Nocentini, S., Buttoud, G., Ciancio, O., Corona, P., 2017. Managing forests in a changing
598 world: the need for a systemic approach. A review. *For. Syst.* 26(1), , eR01.

599 Neumann, M., Mues, V., Moreno, A., Hasenauer, H., Seidl, R., 2017. Climate variability
600 drives recent tree mortality in Europe. *Glob Chang Biol.* 23(11), 4788-4797.

601 O'Brien, S. H., Webb, A., Brewer, M.J., Reid, J.B., 2012. Use of kernel density estimation
602 and maximum curvature to set Marine Protected Area boundaries: Identifying a
603 Special Protection Area for wintering red-throated divers in the UK. *Biol. Conserv.*,
604 156, 15-21.

605 O'Quigley, J., Stare, J., 2002. Proportional hazards models with frailties and random
606 effects. *Stats. Med.* 21(21), 3219–3233.

607 Pinheiro, J.C. Bates, D.M., 2000 *Mixed-Effects Models in S and S-PLUS*. Springer, New
608 York.

609 Pinheiro, J., Bates, D., DebRoy, S., Sarkar, D., 2014. *nlme: Linear and Nonlinear Mixed*
610 *Effects Models*. R package version 3, 1-117.

611 Potter, K.M., Conkling, B.L., 2017. *Forest health monitoring: national status, trends, and*
612 *analysis 2016*. Gen. Tech. Rep. SRS-222. Asheville, NC: US Department of
613 Agriculture, Forest Service, Southern Research Station.

614 R Core Team. 2020. *R: A language and environment for statistical computing*. R
615 Foundation for Statistical Computing, Vienna, Austria.

616 Rediam, 2020 *Red de Información Ambiental de Andalucía*, Junta de Andalucía.
617 <http://www.juntadeandalucia.es/medioambiente/site/rediam/menuitem>.

618 Sánchez, M.E., Luchi, N., Jiménez, J.J., De Vita, P., Sánchez, J.E., Trapero, A., Capretti,
619 P., 2007. An isolated population of *Heterobasidion abietinum* on *Abies pinsapo* in
620 Spain. For. Pathol. 37(5), 348-356.

621 Sánchez-Cuesta, R., Ruiz-Gómez, F.J., Duque-Lazo, J., González-Moreno, P., Navarro-
622 Cerrillo, R.M., 2021. The environmental drivers influencing spatio-temporal dynamics
623 of oak defoliation and mortality in dehesas of Southern Spain. Forest Ecol. Manag.
624 485, 118946.

625 Sánchez-Salguero, R., Camarero, J.J., Carrer, M., Gutiérrez, E., Alla, A.Q., Andreu-
626 Hayles, L., Hevia, A., Koutavas, A., Martínez-Sancho, E., Nola, P., Papadopoulos, A.,
627 Pasho, E., Toromani, E., Carreira, J.A. and Linares, J.C., 2017. Climate extremes and
628 predicted warming threaten Mediterranean Holocene firs forests refugia. PNAS,
629 E10142-E10150.

630 Sánchez-Salguero, R.; Navarro-Cerillo, R.M.; Camarero, J.J.; Fernández-Cancio, A.
631 2012. Selective drought-induced decline of pine species in southeastern Spain. Clim.
632 Chang., 113, 767-785.

633 Seidling, W., 2019. Forest monitoring: Substantiating cause-effect relationships. Sci.
634 Total Environ. 687, 610-617.

635 Senf, C., Pflugmacher, D., Zhiqiang, Y., Sebald, J., Knorn, J., Neumann, M., Seidl, R.,
636 2018. Canopy mortality has doubled in Europe's temperate forests over the last three
637 decades. Nat. Commun. 9(1), 1-8.

638 Teshome, D.T., Zharare, G.E., Naidoo, S., 2020. The Threat of the Combined Effect of
639 Biotic and Abiotic Stress Factors in Forestry Under a Changing Climate. Front. Plant
640 Sci. 11, 601009.

641 Therneau, T.M., Grambsch, P.M., 2000. Modeling Survival Data: Extending the Cox
642 Model, Statistics for Biology and Health. Springer-Verlag, New York.

- 643 Trumbore, S., Brando, P., Hartmann, H., 2015. Forest health and global change. *Science*
644 349, 814–818.
- 645 van Mantgem, P.J., Stephenson, N.L., 2007. Apparent climatically induced increase of
646 tree mortality rates in a temperate forest. *Ecol. Lett.*, 10 (10), 909-916.
- 647 Vicente-Serrano, S.M., Beguería, S., López-Moreno, J.I., 2010. A multiscalar drought
648 index sensitive to global warming: the Standardized Precipitation Evapotranspiration
649 Index. *J Clim.* 23, 1696–1718.
- 650 Wandresen, R.R., Netto, S.P., Koehler, H.S., Sanquetta, C.R., Behling, A., 2019.
651 Nonparametric method: Kernel density estimation applied to forestry data. *Floresta*
652 49(3), 561-570.
- 653 Zuur, A.F., Ieno, E.N., Elphick, C.S., 2010. A protocol for data exploration to avoid
654 common statistical problems. *Methods Ecol. Evol.* 1, 3–14.

Figures

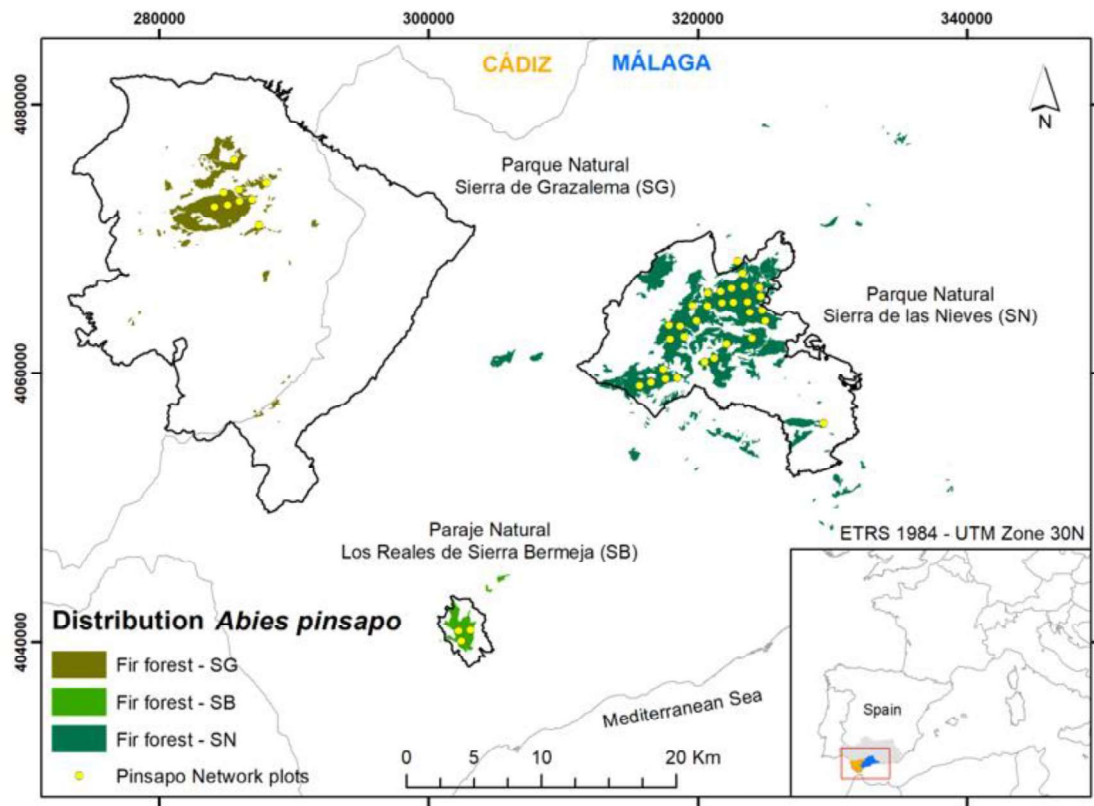


Figure 1. Location of the three major mountain ranges (sierras) where *Abies pinsapo* stands are located in south-eastern Spain (Sierra Bermeja, Sierra de Grazalema and Sierra de las Nieves).

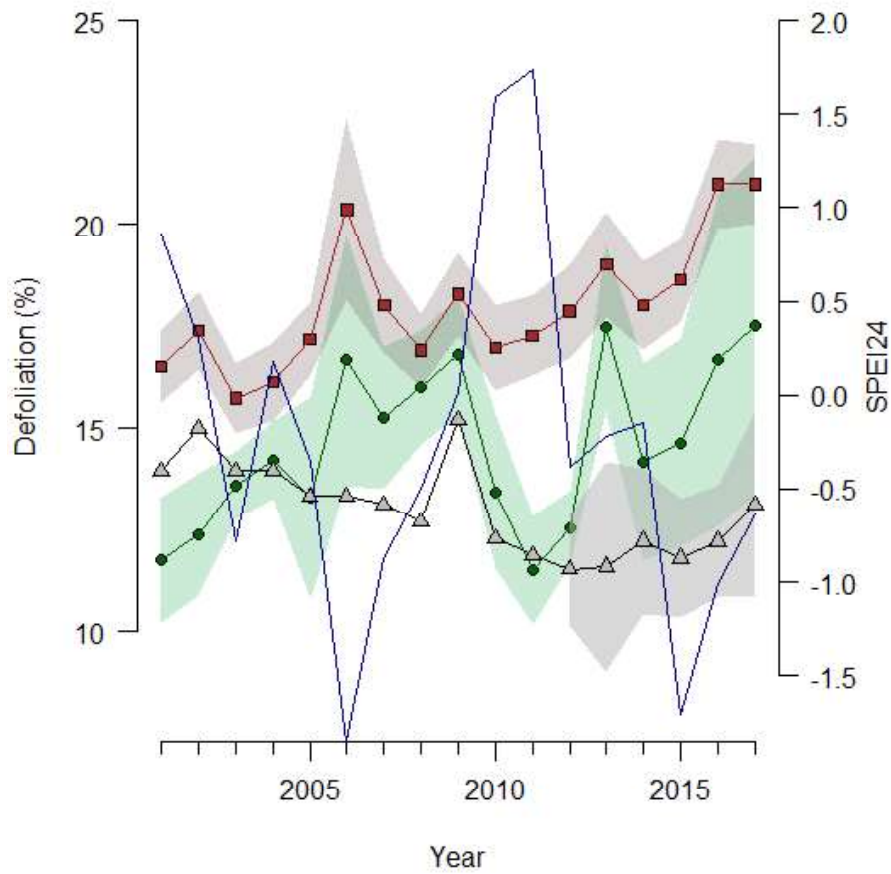


Figure 2. Defoliation trends of *Abies pinsapo* in Sierra de Grazalema (green line), Sierra Bermeja (black line) and Sierra de las Nieves (red line). The solid lines and dots represent the average defoliation while the shaded area represents the standard error for the mean (\pm SE). The solid blue line shows the drought index (average SPEI) in the Sierra de las Nieves site.

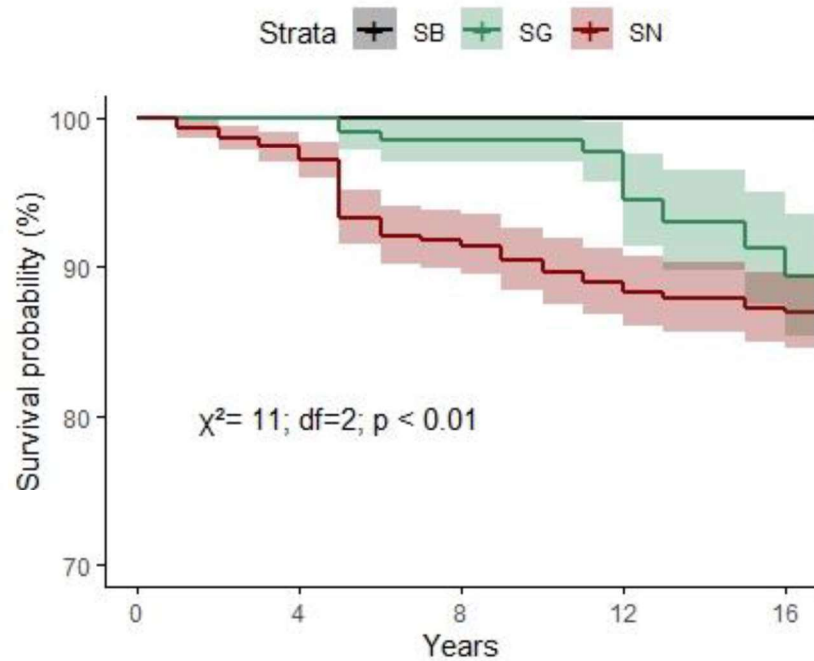
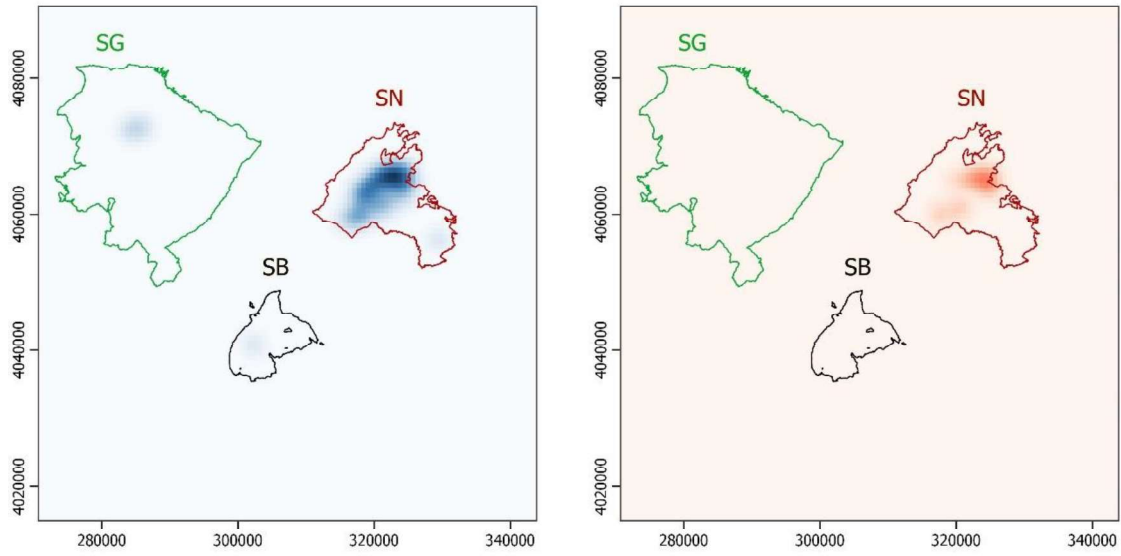


Figure 3. Survival probability graph of *Abies pinsapo* using Kaplan-Meier mortality estimation for the three main distribution locations (SB, Sierra Bermeja, black line; SG, Sierra de Grazalema, green line; SN, Sierra de las Nieves, red line). X-axis, years since the beginning of the monitoring of the health status of the trees on the study plots (2001-2017); Y-axis, proportion of surviving trees (survival rate). The shaded area indicates the standard error of the estimate for each location.

2001



2017

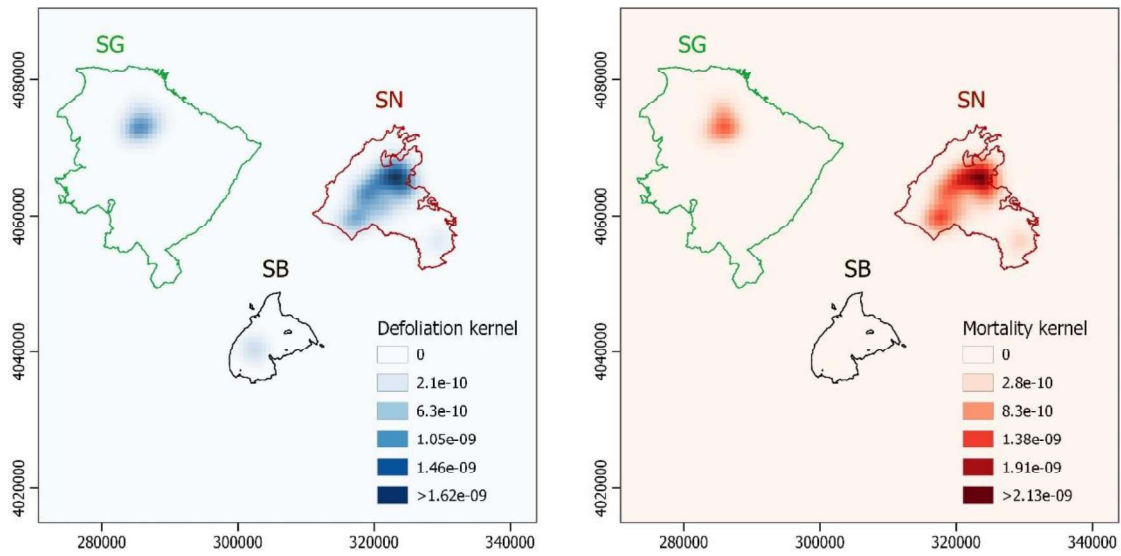


Figure 4. Kernel density analysis of *A. pinsapo* defoliation rate (left, percent defoliation over 24 trees per plot; adimensional density scale) and mortality (right, adimensional density scale) in 2001 (top) and 2017 (bottom) across the species distribution area based on a Kernel density model. X and Y axis showed longitude and latitude respectively (CRS: ETRS89 / UTM 30N)

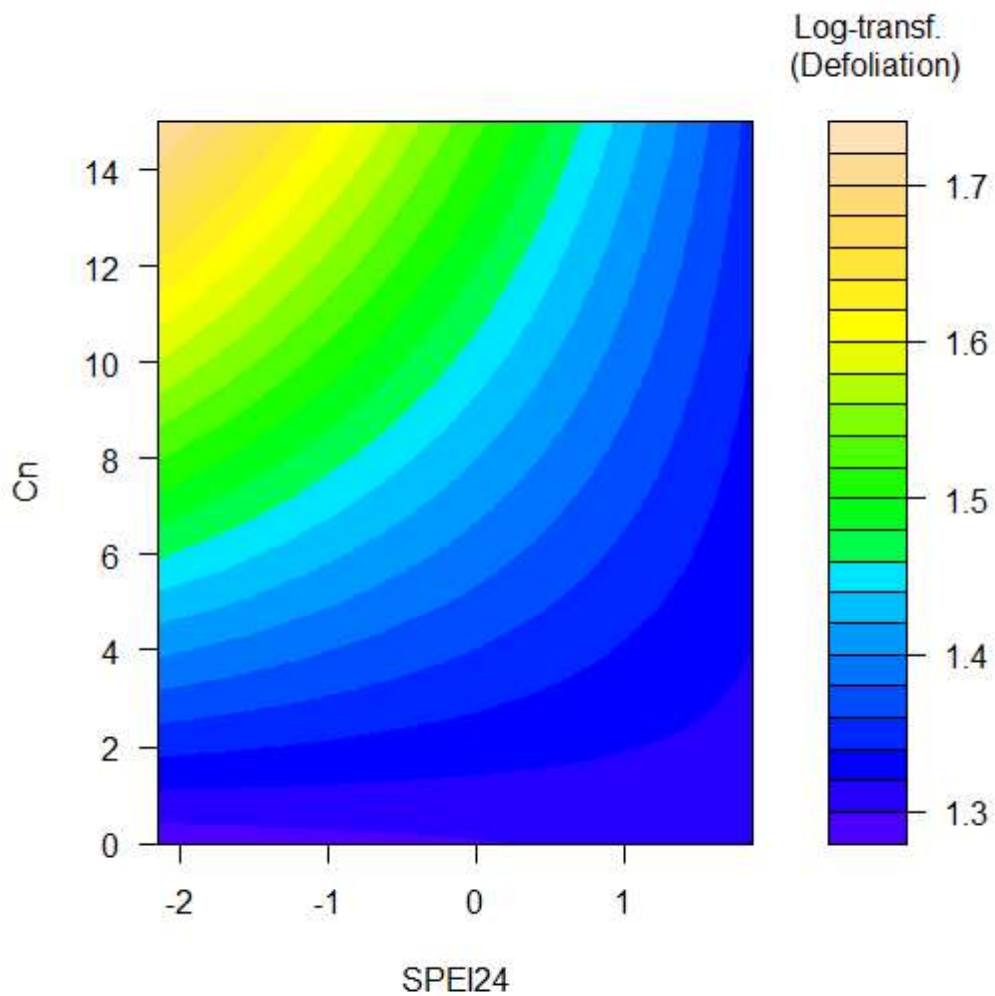


Figure 5. Defoliation rate increased as a function of long droughts (quantified as the Standardised Precipitation-Evapotranspiration Index-SPEI24 for the 24-month period, x axis) and pest severity expressed as number of trees damaged by *Cryphalus numidicus* (Cn) (y axis).

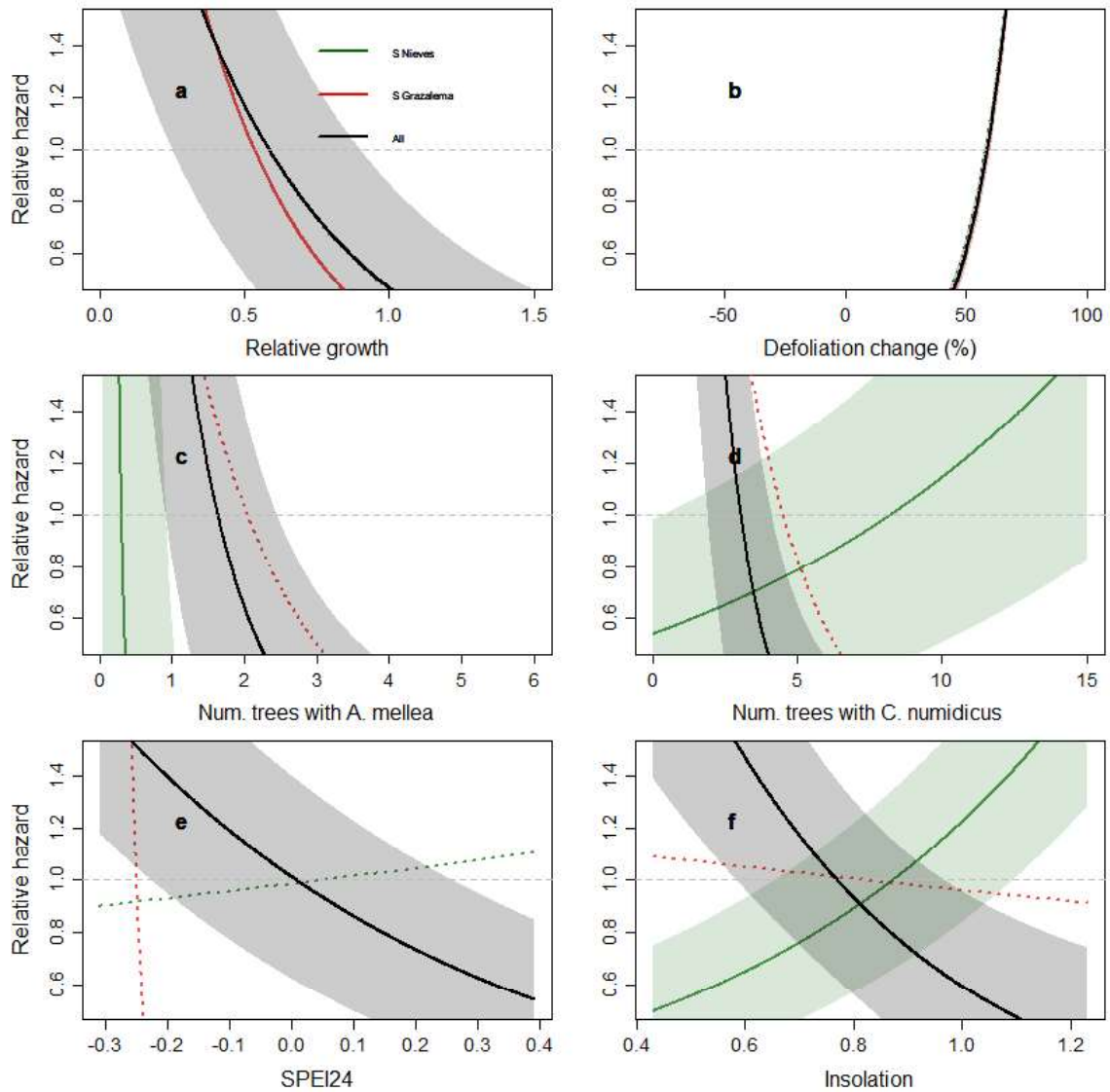


Figure 6. Risk factors identified in the Cox proportional hazard models predicting tree mortality across *Abies pinsapo* forests for all the study area (black line) and the two areas with more mortality: Sierra de las Nieves (green line), and Sierra de Grazalema (red line). Shaded areas represent the standard error for each coefficient and dotted lines represent non-significant risk factors. Selected explanatory variables include relative stem diameter growth rates, defoliation rate between 2001 and 2017, pest severity expressed as number of trees damaged by *Armillaria mellea* and *Cryphalus numidicus*, and drought severity represented as the average of Standardised Precipitation-Evapotranspiration Index (SPEI24) for a 24-month period.

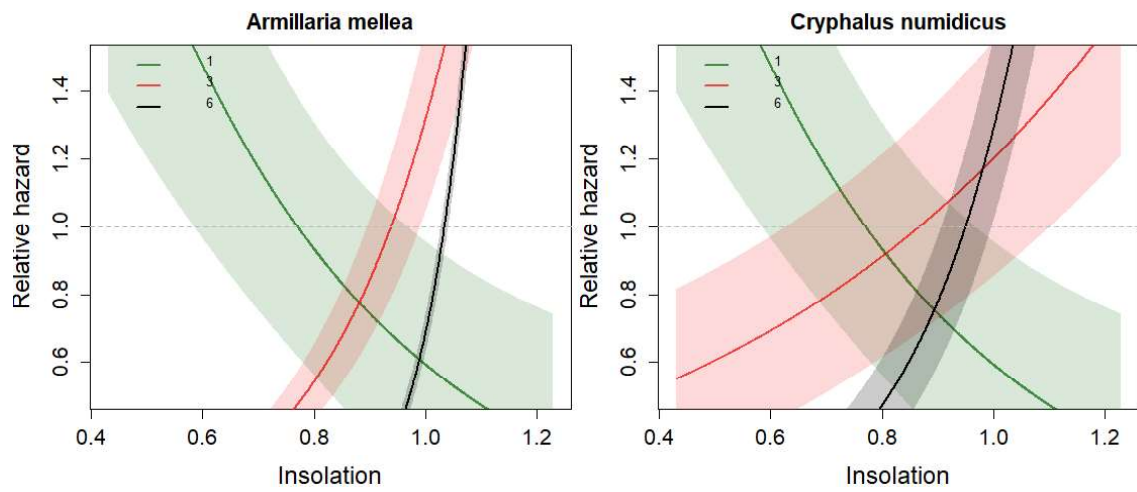


Figure 7. Interaction between abundance two agents (*Armillaria mellea* and *Cryphalus numidicus*) and insolation to predict tree mortality across *Abies pinsapo* forests for all the study area. Shaded areas represent the standard error for each coefficient. Interaction is shown across three levels of abundance (1, 3 and 6 trees infected in the plot),

Table 1. Defoliation model of *Abies pinsapo*. Multimodel inference results of the averaged best models explaining % defoliation (conditional average on models < 7 AICc). Defoliation factors include characteristics from the trees: size, represented by tree diameter at breast height in 2017 (D_{2017}), tree species richness (TDv), relative stem diameter growth rates (RGR); health status: pest severity expressed as number of trees damaged by *Armillaria mellea* (Am), *Cryphalus numidicus* (Cn), and *Dioryctria aulloi* (Da); and site conditions: and site conditions: drought represented as the Standardised Precipitation-Evapotranspiration Index (SPEI24) for the 24-month in the period 2001-2017, insolation (ins), soil depth (ps), slope (pte) and total precipitation (ptt). Interactions between variables are indicated with “:”. In bold, the coefficients that significantly differ from zero ($p < 0.001$).

| | Value | Std.Error | Adjusted SE | z value | Pr(> z) |
|---------------------|---------------|--------------|--------------|--------------|--------------|
| All locations | | | | | |
| (Intercept) | 1.159 | 0.186 | 0.186 | 6.223 | 0.000 |
| Cn | 0.010 | 0.007 | 0.008 | 1.281 | 0.200 |
| Da | -0.047 | 0.026 | 0.027 | 1.759 | 0.079 |
| D_{2017} | 0.001 | 0.001 | 0.001 | 1.180 | 0.238 |
| RGR | -0.138 | 0.093 | 0.096 | 1.436 | 0.151 |
| SPEI24 | -0.008 | 0.014 | 0.014 | 0.574 | 0.566 |
| Cn: SPEI24 | -0.005 | 0.001 | 0.001 | 3.682 | 0.000 |
| D_{2017} : SPEI24 | 0.000 | 0.000 | 0.000 | 1.860 | 0.063 |
| ps | -0.001 | 0.001 | 0.001 | 0.813 | 0.416 |
| ptt | 0.000 | 0.000 | 0.000 | 0.824 | 0.410 |
| TDv | 0.030 | 0.045 | 0.046 | 0.664 | 0.507 |
| Am | 0.009 | 0.023 | 0.024 | 0.393 | 0.694 |
| Di: SPEI24 | -0.003 | 0.007 | 0.007 | 0.505 | 0.614 |
| ins | -0.022 | 0.115 | 0.119 | 0.188 | 0.851 |
| pte | 0.000 | 0.004 | 0.004 | 0.072 | 0.943 |
| ptt: SPEI24 | 0.000 | 0.000 | 0.000 | 0.122 | 0.903 |
| Am: SPEI24 | 0.001 | 0.005 | 0.005 | 0.177 | 0.860 |

Table 2. Comparison between different Cox proportional hazard models predicting tree mortality across *Abies pinsapo* forests. Models are sorted according to AIC values.

| Tree-level attributes | Health status | Site condition | AIC | Wald test | Model description |
|--------------------------|-------------------------------|------------------------|------|-----------|----------------------|
| RGR*** | $\Delta DF^{***} + Am^*$ | SPEI24 ***+ins | 1064 | 297.7*** | Full model |
| | $\Delta DF^{***} + Am + Cn^*$ | | 1119 | 579.7*** | Health status only |
| $D_{2017}^* + RGR^{***}$ | | | 1300 | 133.1*** | Tree-level only |
| | | SPEI24 + ps+pte+ins | 1596 | 0.54 | Site conditions only |

Models vary according to risk factors considered, including tree-level characteristics: tree size, represented by tree diameter at breast height in 2017 (D_{2017}) and relative stem diameter growth rates (RGR), health status: defoliation rate between 2001 and 2017 (ΔDF), pest severity expressed as number of trees damaged by *Armillaria mellea* (Am), and *Cryphalus numidicus* (Cn); and site conditions: drought represented as the average of Standardised Precipitation-Evapotranspiration Index (SPEI24) for the 24month period, insolation (ins), soil depth (ps), slope (pte) and total precipitation (ptt). Significance levels: ***: $p < 0.001$, *: $p < 0.05$.

Table 3. Coefficients from the best (lowest AIC) Cox proportional hazard model of *Abies pinsapo* tree mortality for the full model and with mortality including interactions (“:”) between biotic agents (*Armillaria mellea* (Am) and *Cryphalus numidicus* (Cn)) and the rest of variables.

| | coef | exp(coef) | se(coef) | robust se | z | Sig. |
|---------------------------|-------|-----------|----------|-----------|-------|------|
| All sites (n=1023, d=117) | | | | | | |
| RGR | -1.85 | 0.16 | 0.79 | 0.51 | -3.64 | *** |
| Am | -1.21 | 0.30 | 0.63 | 0.38 | -3.21 | ** |
| Cn | -0.81 | 0.44 | 0.30 | 0.21 | -3.92 | *** |
| Δ DF | 0.06 | 1.06 | 0.00 | 0.00 | 11.89 | *** |
| SPEI24 | -1.62 | 0.20 | 0.52 | 0.62 | -2.60 | ** |
| ins | -2.28 | 0.10 | 1.29 | 1.12 | -2.05 | * |
| RGR:Cn | -0.40 | 0.67 | 0.24 | 0.20 | -2.00 | * |
| Cn:ins | 1.22 | 3.39 | 0.40 | 0.30 | 4.04 | *** |
| Am:ins | 2.24 | 9.43 | 1.02 | 0.62 | 3.63 | *** |

For each risk factor selected in the best model we provide the coefficient (coef), its standard error (SE), exponent (exp(coef)), and statistical significance (*** <0.0001 , ** <0.001 , * <0.05). Risk factors include: stem diameter growth rates (RGR), defoliation rate between 2001 and 2017 (Δ DF), number of trees damaged by *Armillaria mellea* (Am) and *Cryphalus numidicus* (Cn), drought represented as the average of Standardised Precipitation-Evapotranspiration Index (SPEI24) for the 24-month period and insolation (ins). The number of trees included in the analysis (n) and the number of dead trees (d) are shown.

Conflicts of Interest: The authors declare no conflict of interest.

FORECO-D-21-01083

“Drought stress and pests increase defoliation and mortality rates in vulnerable *Abies pinsapo* forests ”

Journal: Forest Ecology and Management

Author Statement

All persons who meet authorship criteria are listed as authors, and all authors certify that they have participated sufficiently in the work to take public responsibility for the content, including participation in the concept, design, analysis, writing, or revision of the manuscript. Furthermore, each author certifies that this material or similar material has not been and will not be submitted to or published in any other publication before its appearance in Forest Ecology and Management.

Authorship contributions

Conceptualization, Rafael M. Navarro-Cerrillo; Methodology, Rafael M^a Navarro-Cerrillo, Francisco José Ruiz-Gómez, Pablo González-Moreno, Rafael Sánchez de la Cuesta, Jesús J Camarero; Formal Analysis, Rafael M^a Navarro-Cerrillo, Pablo González-Moreno, Francisco José Ruiz-Gómez, Antonio Gazol; Writing—Original Draft Preparation, Rafael M^a Navarro-Cerrillo, Pablo González-Moreno, Francisco José Ruiz-Gómez, Writing—Review & Editing, All authors. All authors have read and agreed on the published version of the manuscript.

On behalf of the authors

Rafael M^a Navarro-Cerrillo, PhD

Professor, Department of Forestry

University of Córdoba-Spain

On behalf of the authors



Click here to access/download
Supplementary Material
renamed_ecfa7.docx

